FOUNDATIONS
ADVANCES

ISSN: 2053-2733
journals.iucr.org/a

# An accurate theory of X-ray coplanar multiple SRMS diffractometry

**V. G. Kohn**

*Acta Cryst.* (2018). A**74**, 673–680

FOUNDATIONS ADVANCES

ISSN 2053-2733

# An accurate theory of X-ray coplanar multiple SRMS diffractometry

**V. G. Kohn***

National Research Centre 'Kurchatov Institute', Kurchatov square 1, 123182 Moscow, Russia. *Correspondence e-mail: kohnvict@yandex.ru

Received 25 May 2018
Accepted 5 September 2018

Edited by L. D. Marks, Northwestern University, USA

**Keywords:** X-ray diffraction; silicon crystal; multiple diffraction; synchrotron radiation; slit diffraction.

The article reports an accurate theory of X-ray coplanar multiple diffraction for an experimental setup that consists of a generic synchrotron radiation (SR) source, double-crystal monochromator (M) and slit (S). It is called for brevity the theory of X-ray coplanar multiple SRMS diffractometry. The theory takes into account the properties of synchrotron radiation as well as the features of diffraction of radiation in the monochromator crystals and the slit. It is shown that the angular and energy dependence (AED) of the sample reflectivity registered by a detector has the form of a convolution of the AED in the case of the monochromatic plane wave with the instrumental function which describes the angular and energy spectrum of radiation incident on the sample crystal. It is shown that such a scheme allows one to measure the rocking curves close to the case of the monochromatic incident plane wave, but only using the high-order reflections by monochromator crystals. The case of four-beam (220)(331)($\overline{1}\overline{1}$1) diffraction in Si is considered in detail.

## 1. Introduction

The phenomenon of X-ray monochromatic plane-wave multiple diffraction in single crystals was predicted by Ewald in 1917 (Authier, 2005; Chang, 2004; Pinsker, 1978). However, a detailed study of this phenomenon only became possible many years later. The reason for this is the rather complex nature of this effect: the strong interaction of several plane waves inside the crystal should be described by matrix algebra without the possibility of obtaining an analytical solution in a general case. Therefore computer simulations are necessary.

At the same time, the weak interaction of X-ray radiation with matter is a reason why this effect occurs in very narrow regions in angular and frequency domains. To observe plane-wave multiple diffraction a strong angular collimation in two directions and a strong monochromatization up to the values of $10^{-6}$ are necessary. That is why for many years theoretical and experimental investigations were performed independently. For example, the effect of a strong decrease in the absorption of a part of the X-ray radiation in the six-beam case, which was predicted by Joko & Fukuhara (1967) and discussed by Afanas'ev & Kohn (1977), has not been clearly observed experimentally up to now.

The coincidence of theoretical and experimental results was obtained recently in investigating the effect of total reflection of the X-ray monochromatic plane wave in the forbidden diffraction direction in the three-beam case (Kazimirov & Kohn, 2010, 2011) and four-beam case (Kohn & Kazimirov, 2012). In these works many crystals with high-order reflections were used to obtain a strongly monochromatic and collimated beam of synchrotron radiation. Although an effect was predicted theoretically 22 years before the experiment (Kohn,

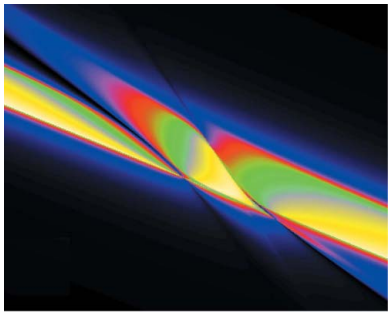

1988*a*,*b*) it was impossible to perform an experimental study earlier.

However, a wide spectrum of synchrotron radiation allows one to use a simpler experimental setup if the coplanar case of X-ray multiple diffraction is under consideration. Coplanar multiple diffraction (CMD) occurs when a wavevector of the incident monochromatic plane wave $\mathbf{k}_0$ and wavevectors of all diffracted waves $\mathbf{k}_m = \mathbf{k}_0 + \mathbf{h}_m$ lie on the same plane and are the radii of some circle in the plane of reciprocal space (Chang, 2004). In this case, all atomic planes inside the crystal which reflect a plane wave are normal to one plane which can be determined by the unit vector $\mathbf{n}_0$ as the vector normal to this plane. In other words, all the reciprocal-lattice vectors of multiple diffraction $\mathbf{h}_m$ lie on the same plane and make an angle of 90° with $\mathbf{n}_0$.

It is evident that this is possible only for the well defined energy $E_0 = \hbar\omega_0 = \hbar cK$ of X-ray photons where $K = |\mathbf{k}_n| = 2\pi/\lambda$, $\hbar = h/2\pi$, $h$ is the Planck constant, $c$ is the light velocity, $\lambda$ is the wavelength. Such an energy can be easily selected from the synchrotron radiation spectrum. In this case the intensity of diffracted beams depends weakly on the angular deviation of the direction of the incident plane wave in the plane normal to the plane of CMD and this dependence can be neglected. Therefore a strong collimation only for one angle inside the plane of CMD is necessary together with monochromatization of radiation.

In this work we demonstrate that the experimental setup shown in Fig. 1 may be successful in several cases of CMD. This experimental setup is rather simple. It consists of a generic synchrotron radiation (SR) source, double-crystal monochromator (M) and slit (S) in the same plane normal to the beam. The method exploring this experimental setup can be called for brevity SRMS diffractometry. We assume that all crystals have the form of a plane parallel plate.

Such a setup was used by Blagov *et al.* (2011) for studying the coplanar X-ray three-beam diffraction in a $TeO_2$ single crystal using the Kurchatov Synchrotron Radiation Source (Moscow). The experimental curves of angular dependence of a weak, strongly asymmetric reflection were found to be much wider than the theoretical plane-wave curves. However, detailed analysis of the instrumental functions was not performed. We note that some theoretical calculations of the instrumental function in the diffractometry experiments were made earlier (Boulle *et al.*, 2002; Kaganer *et al.*, 2001; Mikhalychev *et al.*, 2015; Río & Dejus, 2011). However, an accurate account of the diffraction of synchrotron radiation on the slit has not been given before.

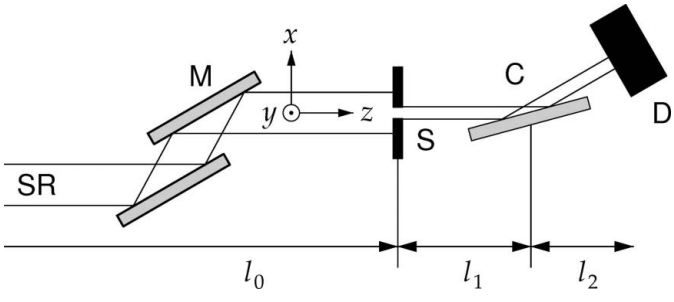


**Figure 1**
A scheme of the SRMS experimental setup. SR is the synchrotron radiation beam, M is the monochromator, S is the slit, C is the sample crystal and D is the detector. The $z$ axis is always along the beam, the $x$ axis is normal to the beam in the plane of CMD and the $y$ axis is normal to the plane of CMD.

The setup shown in Fig. 1 makes a theoretical calculation difficult because the X-ray diffraction on the slit has to be considered in real space while the diffraction in the crystals has to be considered in reciprocal space. Therefore, a transition from real space to reciprocal space and *vice versa* is necessary. Another problem is that the source size and properties of the source radiation strongly influence the result. We used the model of the synchrotron radiation source in which transverse distribution in space of independent point monochromatic radiators is considered.

The reason for choosing this model is the fact that the observation time in a typical experiment is much longer than the duration of radiation from individual electrons inside the bunch. Therefore, the phase relations between such individual flashes of radiation are absent. In this case one has to calculate the intensity at the detector from the radiation of a point monochromatic radiator. Then one has to perform a convolution of this intensity distribution with transverse distribution in space of the source intensity as well as with the radiation spectrum function.

The case of four-beam (220, 331, $\overline{1}\overline{1}1$) coplanar X-ray diffraction in a Si single crystal was used as an example for applying the developed theory. To the best of the author's knowledge, this case has not been investigated before. It is shown that the use of high-order reflections in the monochromator crystals allows one to observe the rocking curve for a monochromatic incident plane wave.

## 2. An accurate theory of CMD in the SRMS experimental setup

The direction of the electric field vector of SR is well determined and stays the same in the CMD experiments. Therefore it is sufficient to consider the scalar wavefunction as the amplitude of the electric field vector. It is known that the beam of SR is well collimated, and it has small transverse sizes as compared with the distance along the beam. In the middle part of the transverse section of the beam the scalar wavefunction of monochromatic radiation can be approximated as a spherical wave in paraxial approximation:

$$\psi(x, y, z, \omega) = \exp(iKz - i\omega t)A_0'(x, y, z, \omega), \qquad (1)$$

where a transverse part $A_0'(x, y, z, \omega)$ is described in free space as

$$A_0'(x, y, z, \omega) = \exp\left(i\pi\frac{x^2 + y^2}{\lambda z}\right). \qquad (2)$$

Here $\lambda = 2\pi c/\omega$. The coordinate system is shown in Fig. 1. We choose the $z$ axis along the direction of the beam, the $x$ axis in the plane of CMD and the $y$ axis as the normal to the plane of CMD.

We consider the frequency $\omega$ which is close to the frequency $\omega_0$ at which CMD occurs. In this case the crystals and the slit influence only the $x$ dependence of the function $A'(x, y, z, \omega)$ whereas the $y$ dependence of this function stays the same in the form of the phase factor. Therefore the $y$ dependence of the intensity is absent, and the $y$ coordinate can be excluded from further analysis. Function (1) is written for the point source at $x = 0$. If the point radiator in the SR source transverse section has a coordinate $x_s$ along the $x$ axis, then $x$ has to be replaced by $x - x_s$ in function (2).

Below we omit the $z$ argument because we will consider definite distances along the beam and replace $\omega$ by $q_\omega$ as a relative deviation of the frequency from a definite value. We choose the base trajectory with the beginning at $x_s$. It goes along the $z$ axis up to the surface of the first crystal of the monochromator. Then it is reflected by the angle $2\theta_B$ for the frequency $\omega_1$ which is determined by the angular position of the monochromator, and it goes further up to the surface of the second crystal of the monochromator. Then it is reflected once again by the same angle $2\theta_B$ but in the opposite direction, and it goes along the $z$ axis up to a slit (see Fig. 1).

Because of the weak interaction of X-ray radiation with matter it is sufficient to consider small deviations in the directions of plane-wave components and small shifts of frequency from the value $\omega_1$. In front of the slit we can write the transverse part of the radiation wavefunction as

$$A'_0(x, q_\omega) = \int \frac{dq}{2\pi} \exp(iqx) P_M^2(q + C_1 q_\omega) P(q, l_0). \quad (3)$$

Here $q = |\mathbf{q}|$, the vector $\mathbf{q}$ being normal to the unit vector $\mathbf{e}_0$ along the $z$ axis. It describes the angular deviation of the plane-wave component with the wavevectors $\mathbf{k} = \mathbf{e}_0 K + \mathbf{q}$ in an integral representation of the wavefunction [see equation (1)] over plane waves. If the angular position of the monochromator corresponds to the frequency $\omega_1$ then $\mathbf{e}_0 K_1 + \mathbf{h} = \mathbf{e}_h K_1$ where $K_1 = \omega_1/c$, $\mathbf{e}_h$ is the unit vector along the base trajectory between the crystals, and $\mathbf{h}$ is the reciprocal-lattice vector for a reflection in the first monochromator (FM) crystal. We assume that a scalar product $\mathbf{qh}$ has a negative value.

Then we can write $K = K_1(1 + \Delta\omega/\omega_1)$ and consider $\Delta\omega/\omega_1$ as a small value because the experimental setup restricts the possible values of $\Delta\omega = \omega - \omega_1$. On the other hand, the $\omega_1$ can have an arbitrary value inside the wide SR spectrum. The phase factor $\exp(iKz)$ does not influence the intensity and may be excluded from our calculations. Below we will write $\Delta\omega/\omega_1 = \theta_\omega$, where $\theta_\omega$ can be called an effective angle and we will use $q_\omega = K_1\theta_\omega = \Delta\omega/c$. Thus we replace the frequency deviation by the angular deviation or wavenumber deviation.

The reflected plane wave due to diffraction in the FM crystal has a wavevector $\mathbf{k}_h = \mathbf{e}_h K_1 + \mathbf{q} + \mathbf{e}_0 q_\omega + C\mathbf{n}_c$, where $\mathbf{n}_c$ is the unit vector. It is normal to the FM crystal surface and directed inside the crystal. The coefficient $C$ is determined from the condition $|\mathbf{k}_h| = K$. We note that in the case of symmetrical reflection the direction of $\mathbf{n}_c$ is opposite the direction of $\mathbf{h}$. The additional term $C\mathbf{n}_c$ appears due to refraction at the crystal surface.

Inside the crystal the wavevector is $\mathbf{k}'_h = \mathbf{e}_0 K + \mathbf{h} + \mathbf{q}$, and $|\mathbf{k}'_h| = K(1 + \alpha/2)$ where

$$\alpha = \frac{(\mathbf{k}'_h)^2 - K^2}{K^2} = 2\frac{(\mathbf{hq}) + (\mathbf{he}_0)q_\omega}{K^2}. \quad (4)$$

Here we use the equation $|\mathbf{h}|^2 = -2(\mathbf{he}_0)K_1$. The parameter $\alpha$ describes deviation from the Bragg condition. It is small because $q$ and $q_\omega$ are small values and we take into account only linear terms in calculations. We note that the reflection amplitude $P_M = E_h/E_0$ of the plane wave depends just on this parameter (Authier, 2005). Here $E_0$ and $E_h$ are the electric field amplitudes for the incident and reflected plane waves, respectively.

In estimating $\alpha$ within our approximation we can replace $K$ by $K_1$, $h = 2K_1 \sin\theta_B$, the angle between $\mathbf{h}$ and $\mathbf{q}$ is equal to $\theta_B + \pi$, the angle between $\mathbf{h}$ and $\mathbf{e}_0$ is equal to $\theta_B + \pi/2$ and

$$\alpha = -2\sin(2\theta_B)(q + C_1 q_\omega)K_1^{-1},\ C_1 = \tan\theta_B. \quad (5)$$

Therefore $\alpha$ is proportional to $(q + C_1 q_\omega)$ and we write this value in equation (3) as the argument of the reflection amplitude. We write the second degree because of the fact that two crystals reflect the plane wave similarly and restore the initial wavevector $\mathbf{k}$ in the twice-reflected wave. The index 1 in $C_1$ means that the Bragg angle corresponds to the monochromator.

The function

$$P(q, z) = \exp\left(-i\frac{\lambda z}{4\pi}q^2\right) \quad (6)$$

is the Fourier image of the Fresnel propagator as the transverse part of the spherical wave in the paraxial approximation [see, for example, Kohn (2012)]. We note that equation (3) is equivalent to four convolutions which describe five processes: (i) propagation from the point source to the FM crystal, (ii) reflection by the FM crystal, (iii) propagation between the crystals, (iv) reflection by the second crystal, (v) propagation from the second crystal to the slit. The Fourier transformation allows us to simplify the problem. It is evident that the distance $l_0$ in equation (3) is equal to the length of the base trajectory from the point source to the slit.

We note that the Fresnel propagator has to depend on the real photon energy. However, a small relative deviation of the frequency can be compensated by a small relative deviation of the distance. It is known that the result depends weakly on the small relative change of the distance. Therefore, we can use the frequency $\omega_1$ instead of $\omega$. As a result, a strong dependence on the frequency is effectively determined by the parameter $q_\omega$.

The wavefunction behind the slit is equal to

$$A'_1(x, q_\omega, x_s) = A'_0(x, q_\omega)T(x + x_s),\ T(x) = \theta(x_0 - |x|). \quad (7)$$

Here $\theta(x)$ is the Heaviside function which equals unity for a positive argument and zero for a negative argument, $x_0 = d/2$, $d$ is the slit width. We took into account the fact that the slit position is independent of the base trajectory and we deter-

mine this position for $x_s = 0$. Therefore, for any value of $x_s$ we have the same function $A'_0(x, q_\omega)$ but we need to take into account the position of the slit relative to the point source as $-x_s$. We note that rotating the monochromator with the aim of slightly changing the frequency $\omega_1$ can lead to an additional shift of the base trajectory relative to the slit. However this shift is very small and can be neglected.

To describe CMD in the sample crystal we need to represent the wavefunction as a superposition of plane waves,

$$A'_1(x, q_\omega, x_s) = \int \frac{\mathrm{d}q}{2\pi} \exp(iqx) A_1(q, q_\omega, x_s), \tag{8}$$

where

$$A_1(q, q_\omega, x_s) = \int \mathrm{d}x \exp(-iqx) A'_1(x, q_\omega, x_s). \tag{9}$$

Then we can consider all scattering processes: (i) propagation from the slit to the sample crystal, (ii) reflection by the sample crystal, (iii) propagation from the sample crystals to the detector, as a product of scattering amplitudes.

Finally, the wavefunction at the detector can be written as

$$A'_2(x) = \int \frac{\mathrm{d}q}{2\pi} \exp(iqxb) P(qb, l_2) P_C(q_r \pm q, q_{1\omega}) \times P(q, l_1) A_1(q, q_\omega, x_s). \tag{10}$$

Here $l_1$ is the distance between the slit and the sample crystal, $l_2$ is the crystal-to-detector distance, $P_C$ is the reflection amplitude for a specific reciprocal-lattice vector of the CMD. Here we took into account three new peculiarities of the sample reflection.

The first one is that the sample crystal can have two positions which can be called nondispersive and dispersive. In the nondispersive case, the beam reflected by the sample crystal has a direction close to the direction of the beam after the FM crystal reflection. The angle between these beams is equal to $2(\theta_{B2} - \theta_{B1})$. In the dispersive case the angle is $2(\theta_{B2} + \theta_{B1})$. Both cases are specified by the sign in front of $q$. In this work we assume the first case.

The second peculiarity is that the sample crystal can be rotated independently of the monochromator. We take this into account by means of representing the reciprocal-lattice vector as $\mathbf{h} = \mathbf{h}_0 + \mathbf{h}_1$ where $\mathbf{h}_0$ is the value corresponding to the optimum crystal angular position and $\mathbf{h}_1$ is a small vector which is normal to $\mathbf{h}_0$. The rotation angle is equal to $\theta_r = h_1/h_0$. We note that it is useful to count the frequency $\omega$ in the CMD calculations relative to the value $\omega_0$ when all parameters of deviation from the Bragg condition are met simultaneously. Then $(\mathbf{e}_0 K_0 + \mathbf{h}_0)^2 = K_0^2$, $K = K_0 + q_{1\omega}$, where $q_{1\omega} = q_1 + q_\omega$, $q_1 = (\omega_1 - \omega_0)/c$ and

$$\alpha = K_0^{-2}[(\mathbf{e}_0 K_0 + \mathbf{h}_0 + \mathbf{h}_1 + \mathbf{q} + \mathbf{e}_0 q_{1\omega})^2 - K^2] = 2K_0^{-2}[(\mathbf{h}_0\mathbf{q}) + (\mathbf{h}_0\mathbf{e}_0) q_{1\omega} + (\mathbf{h}_1\mathbf{e}_0) K_0]. \tag{11}$$

Now $h_0 = 2K_0 \sin\theta_B$, the angle between $\mathbf{h}_0$ and $\mathbf{q}$ is equal to $\theta_B + \pi$, the angle between $\mathbf{h}_0$ and $\mathbf{e}_0$ is equal to $\theta_B + \pi/2$, and we choose the angle between $\mathbf{h}_1$ and $\mathbf{e}_0$ as $\theta_B + \pi$.

As a result

$$\alpha = -2\sin(2\theta_B)(q + q_r + C_2 q_{1\omega}) K_0^{-1}, \quad C_2 = \tan\theta_B. \tag{12}$$

Here $q_r = K_0\theta_r$. The index 2 in $C_2$ means that the Bragg angle corresponds to the sample reflection. We note that the plus sign in front of $q_r$ is a consequence of our choice of the rotation direction when the angle between the incident wave and the reflecting atomic planes increases due to rotation. In the case of multiple diffraction we have several reflections simultaneously with different values of the Bragg angle. Therefore, the reflection amplitude $P_C(,)$ depends on two arguments $q + q_r$ and $q_{1\omega}$ separately.

The third peculiarity is asymmetry of the sample reflection, *i.e.* the angle between $\mathbf{n}_c$ and $\mathbf{h}_0$ is different from 180°. In this case the crystal changes both the direction of the reflected beam and its angular divergence (Authier, 2005). If the angular deviation of the incident beam is $\theta = q/K_0$, then for the reflected beam the angular deviation from the base trajectory is $\theta' = qb/K_0$, where $b = \sin\theta_0/\sin\theta_h$ and $\theta_0, \theta_h$ are the angles between the crystal surface and the unit vectors $\mathbf{e}_0$, $\mathbf{e}_h$ (Authier, 2005). We note that $\theta_0 + \theta_h = 2\theta_B$. In the symmetrical case $\theta_0 = \theta_h = \theta_B$.

In the method of SRMS diffractometry one measures the integral intensity of radiation at the detector as a function of the rotation angle $\theta_r$ and the angle $\theta_1 = q_1/K_0$ which is determined by the angular position of the monochromator. The integral intensity for the point monochromatic radiator is equal to

$$S_1(p) = \int \mathrm{d}x \left|A'_2(x)\right|^2, \; p = \theta_r, \theta_1, x_s, \theta_\omega. \tag{13}$$

We substitute equation (10) in equation (13) and calculate the integral which gives the following result:

$$S_1(p) = b^{-1} \int \frac{\mathrm{d}q}{2\pi} \left|P_C(q_r + q, q_{1\omega})\right|^2 \left|A_1(q, q_\omega, x_s)\right|^2. \tag{14}$$

Equation (14) is the well known Parseval rule which is formulated as the integral intensities in real and reciprocal spaces are equal to each other. The factor $b^{-1}$ is a consequence of the fact that variables $x$ and $q$ are not fully mutual. Since the Fresnel propagator has a unit modulus the distances $l_1$ and $l_2$ do not influence the integral intensity. It is a consequence of the energy conservation law.

The experimentally measured value is calculated as

$$S(\theta_r, \theta_1) = \int \mathrm{d}x_s G_B(x_s) \int \mathrm{d}\theta_\omega S_1(\theta_r, \theta_1, x_s, \theta_\omega), \tag{15}$$

where $G_B(x_s)$ is the intensity distribution on the source. This function is usually chosen as the Gaussian function:

$$G_B(x_s) = (2\pi)^{-1/2} \sigma_x^{-1} \exp(-x_s^2/2\sigma_x^2). \tag{16}$$

We note that the experimental data are obtained point by point during rotation of the sample crystal and the monochromator crystals. It is convenient to consider the curve of $\theta_r$ dependence for several reflections at the fixed value of $\theta_1$. Such curves are called CDR (curve of diffraction reflection). A set of such curves can be obtained by changing $\theta_1$.

Computer simulations can be performed similarly as a convolution of the monochromatic plane-wave multiple

diffraction data and the instrumental function which can be calculated separately.

## 3. Instrumental function

We substitute equation (14) into equation (15) and change the order of integration as well as replace variable wavenumbers by angles as $\theta = q/K_0$ and so on. We will also omit all constant multipliers general for all reflections because we are interested only in relative values. Under these conditions we have

$$S(\theta_r, \theta_1) \propto \int \mathrm{d}\theta\, \mathrm{d}\theta_\omega H(\theta, \theta_\omega) G_C(\theta_r + \theta, \theta_1 + \theta_\omega), \quad (17)$$

where

$$G_C(\theta, \theta_\omega) = b^{-1} \left| P_C(\theta, \theta_\omega) \right|^2 \quad (18)$$

and

$$H(\theta, \theta_\omega) = \int \mathrm{d}x_s G_B(x_s) \left| A_1(\theta, \theta_\omega, x_s) \right|^2. \quad (19)$$

Equation (17) consists of a double integral over the angular and frequency variables of a product of two functions. One of them $G_C(\theta, \theta_\omega)$ describes the intensity of the reflected beam in the case of CMD of the monochromatic plane wave with given angular and frequency deviations from the values which satisfy all Bragg conditions for the CMD under consideration. The second function $H(\theta, \theta_\omega)$ does not describe the CMD. It describes the weights of various angular and frequency deviations in the effective incident beam because the incident radiation is not a monochromatic plane wave. This function is usually called the instrumental function.

By means of rotating the sample and monochromator, we have the possibility of choosing mean values of angle and frequency of the incident wave which influence the CMD and thus obtaining some effective angular and frequency profiles. These profiles will be close to the results of the theory of the monochromatic plane wave if the instrumental function equals zero out of the small area near the zero point in the two-dimensional area of arguments. Knowledge of the instrumental function allows us to make accurate computer simulations of the experimental data and to predict the difference from the results of the theory of the monochromatic plane wave.

The function $G_C(\theta, \theta_\omega)$ can be calculated by means of the methods of X-ray monochromatic plane-wave multiple diffraction theory, and the CMD is a particular case. We use the computer program which was described by Kohn (1979) and was used in the works of Kazimirov & Kohn (2010, 2011) and Kohn & Kazimirov (2012). The function $H(\theta, \theta_\omega)$ depends completely on the experimental setup, and has not been considered up to now. It is the main result of this work.

We substitute equations (3), (6), (7) into equation (9) and make a shift of the origin in the integral over $x$. As a result, we obtain

$$A_1(q, q_\omega, x_s) = \int \mathrm{d}x T(x) \int \frac{\mathrm{d}q'}{2\pi} P_M^2(q' + C_1 q_\omega) \times \exp\left[ -\frac{i}{2}(rq')^2 + i(q' - q)(x - x_s) \right], \quad (20)$$

where $r = (l_0/K_0)^{1/2}$. The exponential is a strongly oscillating function. We can estimate the integral over $q'$ approximately by means of the stationary phase method (SPM, Jeffreys & Swirles, 1972). In the point $q' = q'_p = q_x - q_s$ the first derivative of the phase is equal to zero, where

$$q_x = \frac{x}{r^2} = K_0\theta_0,\ q_s = \frac{x_s}{r^2} = K_0\theta_s. \quad (21)$$

According to the SPM approximation we replace the function $P_M^2$ by its value at the point $q'_p$, and calculate accurately the integral from the exponential. We omit the multipliers which do not influence the intensity and shape of the curve and write the result in the form

$$A_1(q, q_\omega, x_s) \propto \int \mathrm{d}x T(x) P_M^2(q_x - q_s + C_1 q_\omega) \times \exp\left[ i\frac{x^2}{2r^2} - i(q + q_s)x \right]. \quad (22)$$

One can see that the integral depends effectively on two independent arguments $(C_1 q_\omega - q_s)$ and $(q + q_s)$. If the integral is known for $q_s = 0$ as the function of two arguments $C_1 q_\omega$ and $q$, then the values of $A_1$ for nonzero values of $q_s$ can be obtained by shifting the first argument down and the second argument up. Let us consider the value $q_s = 0$ and use the function of new angular variables,

$$B(\theta, \theta'_\omega) = \int \mathrm{d}x \exp(-iqx) F(x), \quad (23)$$

where

$$F(x) = P_M^2(\theta_0 + \theta'_\omega) \exp\left( iK_0 \frac{x^2}{2l_0} \right) T(x). \quad (24)$$

Here $\theta'_\omega = C_1\theta_\omega$. We note that the reflection amplitude is calculated usually as a function of the angular variable. The angle $\theta_0 = x/l_0$ has a simple physical meaning. It is an angle between the line from the centre of the source to the current point inside the slit and the base trajectory.

The algorithm for calculating the function $B(\theta, \theta'_\omega)$ is rather simple. The function $P_M^2(\theta_0)$ can be calculated separately on the set of points and then interpolated. The parameter $\theta'_\omega$ influences only this function while the $\theta$ dependence is calculated by means of a fast Fourier transform procedure. We are interested in the square modulus of this function. The integral (19) is calculated by means of interpolating the matrix $|B(\theta, \theta'_\omega)|^2$ along the diagonal from top-left to bottom-right corners and integrating the product of this function and the $G_B(\theta_s)$. Finally, transformation from the variable $\theta'_\omega$ to $\theta_\omega$ can be obtained by the interpolation procedure.

## 4. CMD (220, 331, $\overline{1}11$) in Si

As an example of applying the theory we consider the case of four-beam (220, 331, $\overline{1}11$) coplanar X-ray diffraction in a Si

single crystal. The coplanar case exists for the photon energy $E$ = 8.6182 keV. The directions of the incident (000) wavevector and the diffracted wavevectors are shown in Fig. 2(*a*). We assume that the crystal is very thick; therefore only reflected beams (220) and (331) are of interest and can be measured in the experiment.

The function $G_C(\theta, \theta_\omega)$ for each of these two reflections is calculated by means of the standard computer program which was used in the work of Kohn & Kazimirov (2012) and was elaborated according to the theory proposed by Kohn (1979). The general program can be used in the particular case of coplanar diffraction. Therefore,

$$G_{ms}(\theta, \theta_\omega) = \sum_{s'} \left| \sum_j B^{(j)}_{ms'} C_{sj} \right|^2 \tag{25}$$

where $m$ is the index of reflection, $s$ is the index of polarization of the incident beam, $B^{(j)}_{ms}$ is the $j$th complex eigenvector of the dynamical scattering matrix,

$$\sum_{ns'} g^{ss'}_{mn}(\theta, \theta_\omega) B^{(j)}_{ms'} = \varepsilon_j B^{(j)}_{ms}, \tag{26}$$

where

$$g^{ss'}_{mn}(\theta, \theta_\omega) = \frac{K\chi_{mn}}{\gamma_m^{1/2}\gamma_n^{1/2}}(\mathbf{e}_{ms}\mathbf{e}_{ns'}) - K\alpha_m\delta^{ss'}_{mn}. \tag{27}$$

Here $\chi_{mn}$ is the Fourier image of the susceptibility of the crystal on the reciprocal-lattice vector $\mathbf{h}_m - \mathbf{h}_n$, $\gamma_m$ is the cosine of the angle between the direction of the $m$th beam and the internal normal to the entrance surface of the crystal plate, $\mathbf{e}_{ms}$ are the unit polarization vectors for the beam $m$, $\delta^{ss'}_{mn}$ is the Kroneker's symbol, and

$$\alpha_m = -2\sin(2\theta_{Bm})[\theta + \tan(\theta_{Bm})\theta_\omega] \tag{28}$$

are the parameters of deviation from the two-beam Bragg conditions for the $m$th beam [see equation (12)]. The two-beam cases are realized on the lines parallel to the lines $\alpha_m = 0$ if the point $(\theta, \theta_\omega)$ is far from the central point (0, 0) on the plane of two variables. Some shift takes place due to dynamical phenomena.

The coefficients $C_{sj}$ are the solution of the set of equations

$$\sum_j B^{(j)}_{ms'} C_{s'j} = \delta^{ss'}_{m0}, \tag{29}$$

where only part of the eigensolutions with $\mathrm{Im}(\varepsilon_j) > 0$ is taken into account, and index $m$ runs only over the beams with $\gamma_m > 0$.

Fig. 2(*b*) shows the lines of two-beam diffraction inside the rectangular area in which results of accurate calculation of diffracted (220) and (331) reflectivities are shown in Fig. 3 as a colour map. We consider the case of the $\pi$-polarized incident beam with a direction normal to the scattering plane which is a vertical plane for which the source has a minimum size. The same polarization state remains for all diffracted waves.

It is known that the curve of angular or energy dependence of reflectivity in the case of two-beam diffraction has a shape with a wide maximum like a plateau. Sometimes such a curve is called the Darwin table (Ignatovich *et al.*, 1996). In the plane $(\theta_\omega, \theta)$ the reflectivity is close to unity inside the stripe of some width. One of the effects of multiple diffraction consists of changing the width of this stripe near the multiple diffraction point of the intersection of two beamlines.

This effect was first considered by Høier & Marthinsen (1983) and was explained as a renormalization of the kinematical diffraction parameters due to a process of the second-order scattering from the incident beam to the other beam and then from the other beam to the beam under consideration. The effect is asymmetric, *i.e.* the width becomes wider on one side and narrower on the other side. In Fig. 3 this effect is clearly seen for the (331) beam.

Another effect is a weak excitement of the reflectivity in the area outside the region of the two-beam stripe, but inside the two-beam stripe of the other beam. Inside the area of strong multiple diffraction the reflectivity can be greatly altered and the processes are not simple. For example, the results of

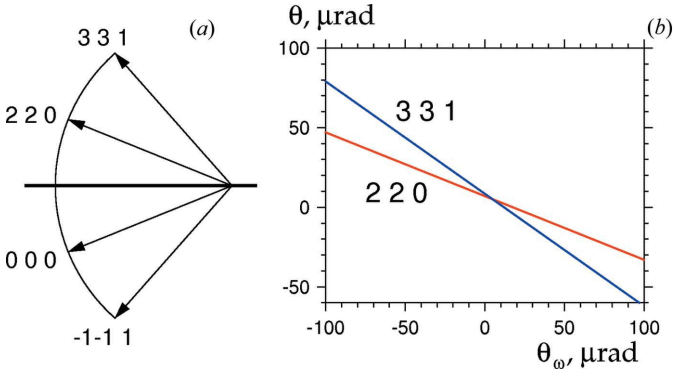


**Figure 2**
(*a*) Directions of the incident (000) and reflected wavevectors, and the crystal surface is shown by a thick horizontal line; (*b*) the area in the $(\theta_\omega, \theta)$ plane for the images in Fig. 3, and the lines of two-beam diffraction.

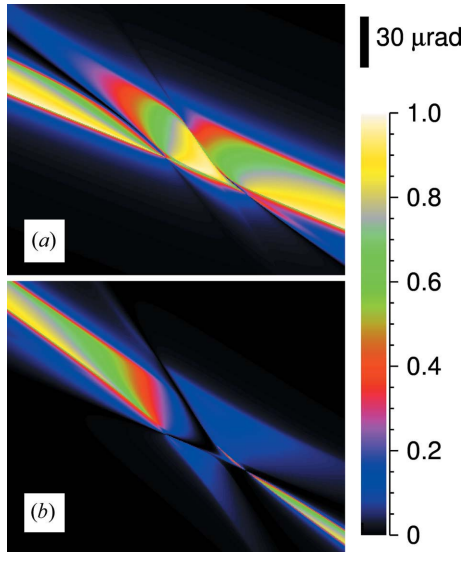


**Figure 3**
The reflectivity distribution in the plane $(\theta_\omega, \theta)$ for the (220) reflected beam (*a*) and (331) reflected beam (*b*). The axes are as shown in Fig. 2.

calculation show that the (331) beam is not reflected in this area while the area of (220) reflectivity has sharp boundaries.

It is impossible to observe the results shown in Fig. 3 in an experiment because the experimental setup allows one to see only a convolution of these distributions with the instrumental function. Let us consider first the parameters of the Kurchatov Synchrotron Radiation Source (KSRS) in Moscow. Then $\sigma_x$ = 54 μm, $l_0$ = 13 m, $x_0$ = 50 μm. Very often the monochromator is made from Si and it is used with a (111) reflection.

The results of calculation of the instrumental function for the parameters listed above are shown in Fig. 4(*a*) in the same units as in Fig. 3. The colour map is also the same but the function is normalized to the unit area. By means of rotating the sample crystal we can calculate the rocking curves, *i.e.* the $\theta_r$ dependence of reflectivity for various values of $\theta_1$. The calculation is performed according to equation (17).

The main result of calculation is shown in Figs. 4(*b*), 4(*c*) and 4(*d*) for $\theta_1$ = 140, 0 and −140 μrad, respectively. The curves 1 (black) and 3 (blue) have to be observed experimentally in the beams (220) and (331), respectively. The instrumental function was taken into account in calculation of these curves. Since these curves are wider and smaller than the rocking curve for a monochromatic plane wave we show them with a height that is twice that of the real height.

For the sake of comparison we show the plane-wave rocking curves 2 (red) and 4 (green) from the data of Fig. 3, *i.e.* the pure profiles without a convolution. The main aim of the multiple diffraction study is to observe just these curves. Our calculations, made according to the developed theory, show that it is impossible in the considered case because the convolution kills the fine details of profiles and makes the curves wider and smoother.

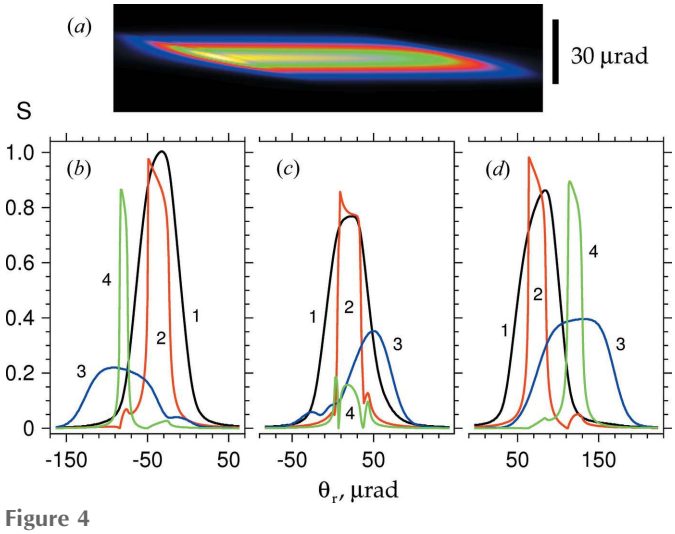


**Figure 4**
(*a*) The instrumental function (IF) $H(\theta_\omega, \theta)$ for the case of the Kurchatov SR source, 100 μm slit size and the Si (111) monochromator as the colour map. The colour scale is the same as in Fig. 3, but the function is normalized on the unit area. (*b*) The $\theta_r$ angular dependence of reflected beam intensities for the $\theta_1$ = 140 μrad; curve 1 (black) is for the (220) beam taking into account a convolution, curve 2 (red) is for the (220) curve on its own (*i.e.* without a convolution), curves 3 (blue) and 4 (green) are the same for the (331) beam. (*c*) and (*d*) are the same for $\theta_1$ = 0 and −140 μrad, respectively. In reality, curves 1 and 3 have a height which is half that shown in the figure. We increase the height to make the curve more visible.

Fig. 4(*a*) shows that the width of the area of the instrumental function (AIF) along the frequency axis $\theta_\omega$ is much larger than along the $\theta$ axis. This peculiarity is the main disadvantage. It is easy to understand from equations (23), (24) that this width is approximately equal to the width of the Darwin table of the monochromator reflectivity along the $\theta_\omega$ axis.

It is known that the width of the Darwin table along the $\theta$ axis is equal to $2|\chi_h|\sin^{-1}(2\theta_B)$ (Authier, 2005). However, it is $\tan^{-1}(\theta_B)$ times wider along the $\theta_\omega$ axis. In our case $|\chi_h|$ = 7.03 μrad, $\theta_B$ = 13.26°, and we obtain an estimate of 133.5 μrad for the width of the AIF along the $\theta_\omega$ axis. Now we understand that we can significantly improve the monochromaticity of the radiation incident on the sample if we use the higher orders of reflection (333) or (444).

The same estimates give the values $|\chi_h|$ = 4.05 μrad, $\theta_B$ = 43.49° for the (333) reflection, and the widths of Darwin tables of 8.11 and 8.55 μrad along the $\theta$ and $\theta_\omega$ axes, respectively. We have performed an accurate calculation for this case and found that the AIF has the shape of a rectangular area as a backwards-sloping diagonal (from top-left to bottom-right) inside a square of 30 μrad side size. The width of this diagonal is about 8 μrad. The additional increase in the AIF size occurs due to the source size and integration in equation (19).

Nevertheless, the sizes of the AIF in this case are sufficiently small and we obtain curves that are very close to the curves 2 and 4 in Fig. 4. The use of the reflection (444) allows one to improve the monochromaticity further. In this case $|\chi_h|$ = 4.19 μrad, $\theta_B$ = 66.59°. We have performed an accurate calculation and found that the AIF looks like a backwards-sloping diagonal inside a rectangular area of 28 μrad height and 12 μrad width. The coincidence with the rocking curves for a monochromatic plane wave improves.

The size of the slit of 100 μm and smaller does not influence significantly the AIF. The smaller size will decrease the intensity of radiation at the detector. The larger size will increase the vertical size along the $\theta$ axis.

Let us estimate the AIF for the typical parameters of the ESRF (Grenoble, France). In this case $\sigma_x$ = 21 μm, $l_0$ = 50 m, and we obtain very good collimation by means of a setup consisting of the source size and the slit. However, with the (111) reflection the incident radiation will not be monochromatic. The width of the AIF along the $\theta_\omega$ axis will be the same as in the above considered case. Therefore the use of high-order reflections is necessary.

## 5. Conclusion

The aim of our work was to show that the effect of coplanar multiple diffraction can be easily investigated using a synchrotron radiation source because it is easy to select the necessary photon energy from the very wide spectrum. In this study a rather simple experimental setup was used which consists of the double-crystal monochromator and a slit of a reasonable size. We developed the theory which allows one to

simulate the experimental rocking curves. The theory takes into account all parameters of the experimental setup such as the source size, the slit size and the monochromator.

We have shown that the rocking curves close to the curves of the theory of the monochromatic plane wave can be obtained even with an SR source of relatively large angular size like the Kurchatov SR source (Moscow). However, it is necessary to use high-order reflections in the monochromator crystals. The same rule has to be fulfilled for a third-generation SR source like the ESRF (Grenoble). The coplanar multiple diffraction is simpler than the general case of multiple diffraction because it takes place inside the plane. On the other hand, high sensitivity to the energy of radiation simultaneously with the angular dependence opens new possibilities to study the structure of solid matter.

## Acknowledgements

The author thanks Ivan Vartaniants for the interest in the work and valuable remarks.

## References

Afanas'ev, A. M. & Kohn, V. G. (1977). *Acta Cryst.* A**33**, 178–184.
Authier, A. (2005). *Dynamical Theory of X-ray Diffraction*, 3rd ed. Oxford University Press.
Blagov, A. E., Koval'chuk, M. V., Kohn, V. G., Mukhamedzhanov, E. Kh., Pisarevsky, Yu. V. & Prosekov, P. A. (2011). *J. Synch. Investig.* **5**, 822–827.
Boulle, A., Masson, O., Guinebretière, R., Lecomte, A. & Dauger, A. (2002). *J. Appl. Cryst.* **35**, 606–614.
Chang, S.-L. (2004). *X-ray Multiple-Wave Diffraction: Theory and Application.* Springer Series in Solid-State Sciences. Berlin: Springer.
Høier, R. & Marthinsen, K. (1983). *Acta Cryst.* A**39**, 854–860.
Ignatovich, V. K., Protopopescu, D. & Utsuro, M. (1996). *Phys. Rev. Lett.* **77**, 4202–4205.
Jeffreys, H. & Swirles, B. (1972). *Methods of Mathematical Physics*, p. 566. Cambridge University Press.
Joko, T. & Fukuhara, A. (1967). *J. Phys. Soc. Jpn*, **22**, 597–604.
Kaganer, V. M., Jenichen, B. & Ploog, K. H. (2001). *J. Phys. D Appl. Phys.* **34**, 645–659.
Kazimirov, A. & Kohn, V. G. (2010). *Acta Cryst.* A**66**, 451–457.
Kazimirov, A. & Kohn, V. G. (2011). *Acta Cryst.* A**67**, 409–414.
Kohn, V. G. (1979). *Phys. Status Solidi A*, **54**, 375–384.
Kohn, V. G. (1988*a*). *Kristallografiya (Moscow)*, **33**, 567–573.
Kohn, V. G. (1988*b*). *Sov. Phys. Crystallogr.* **33**, 333–336.
Kohn, V. G. (2012). *J. Synchrotron Rad.* **19**, 84–92.
Kohn, V. G. & Kazimirov, A. (2012). *Acta Cryst.* A**68**, 331–336.
Mikhalychev, A., Benediktovitch, A., Ulyanenkova, T. & Ulyanenkov, A. (2015). *J. Appl. Cryst.* **48**, 679–689.
Pinsker, Z. G. (1978). *Dynamical Scattering of X-rays in Crystals.* Heidelberg, New York: Springer-Verlag.
Sánchez del Río, M. & Dejus, R. J. (2011). *Proc. SPIE*, **8141**, 814115.